Deep subwavelength beam propagation in extremely loss-anisotropic metamaterials

2013 J. Opt. 15 055105

(http://iopscience.iop.org/2040-8986/15/5/055105)

IOP Publishing Journal of Optics
J. Opt. **15** (2013) 055105 (4pp) doi:10.1088/2040-8978/15/5/055105

Deep subwavelength beam propagation in extremely loss-anisotropic metamaterials

Yingran He[1,2], Lei Sun[1], Sailing He[2] and Xiaodong Yang[1]

[1] Department of Mechanical and Aerospace Engineering, Missouri University of Science and Technology, Rolla, MO 65409, USA
[2] Centre for Optical and Electromagnetic Research, Zhejiang Provincial Key Laboratory for Sensing Technologies, Zhejiang University, Hangzhou 310058, People's Republic of China

E-mail: yangxia@mst.edu

Received 9 January 2013, accepted for publication 25 March 2013
Published 17 April 2013
Online at stacks.iop.org/JOpt/15/055105

Abstract
Metal–dielectric multilayer metamaterials with extreme loss-anisotropy, in which the longitudinal component of the permittivity tensor has an ultra-large imaginary part, are proposed and designed. Diffraction-free deep subwavelength beam propagation and manipulation, due to the nearly flat iso-frequency contour, is demonstrated in such loss-anisotropic metamaterials. It is also shown that deep subwavelength beam propagation can be realized in practical multilayer structures with large multilayer periods, when the nonlocal effect is considered.

Keywords: multilayer metamaterials, extreme loss-anisotropy, deep subwavelength propagation, nonlocal effect

(Some figures may appear in colour only in the online journal)

1. Introduction

Light beams with subwavelength confinement and propagation beyond the diffraction limit are highly desirable for many optical integration applications. To enable the subwavelength optical confinement, optical materials supporting ultra-high wavevectors are necessary. Since the refractive indices of natural materials are quite limited at optical frequency, metamaterials with artificially engineered subwavelength meta-atoms are designed to exhibit ultra-high refractive indices so as to achieve large wavevectors [1, 2]. To obtain diffraction-free deep subwavelength beam propagation, a nearly flat iso-frequency contour (IFC) curve over a broad range in k-space is required, so that all spatial components will propagate with the same phase velocity along the longitudinal direction [3]. Extremely anisotropic metamaterials with an infinite real part of permittivity have been theoretically proposed to achieve flat IFCs and consequently subwavelength beam propagation without diffraction [4, 5].

Recently, metal–dielectric multilayer metamaterials with an indefinite permittivity tensor have been utilized to demonstrate intriguing applications of negative refraction [6], subwavelength imaging [7], enhanced photonic density of states [8], and broadband light absorbers [9], together with ultra-high refractive indices for subwavelength optical waveguides [10] and indefinite cavities [11]. In this work, we propose the concept of extreme loss-anisotropy in metal–dielectric multilayer metamaterials, where the longitudinal component of the permittivity tensor has an ultra-large imaginary part. Diffraction-free deep subwavelength beam propagation and manipulation is demonstrated in such loss-anisotropic metamaterial, due to the nearly flat IFC.

2. Theory and discussion

The inset of figure 1 shows the metal–dielectric multilayer structure, where titanium oxide (Ti_3O_5) with a dielectric constant of 5.83 and silver (Ag) are chosen [12]. When the thickness of each layer is infinitely small, the multilayer structure can be regarded as an anisotropic effective medium with a permittivity tensor of

$$\varepsilon_x = f_d\varepsilon_d + f_m\varepsilon_m, \qquad \varepsilon_y = (f_d/\varepsilon_d + f_m/\varepsilon_m)^{-1}, \quad (1)$$

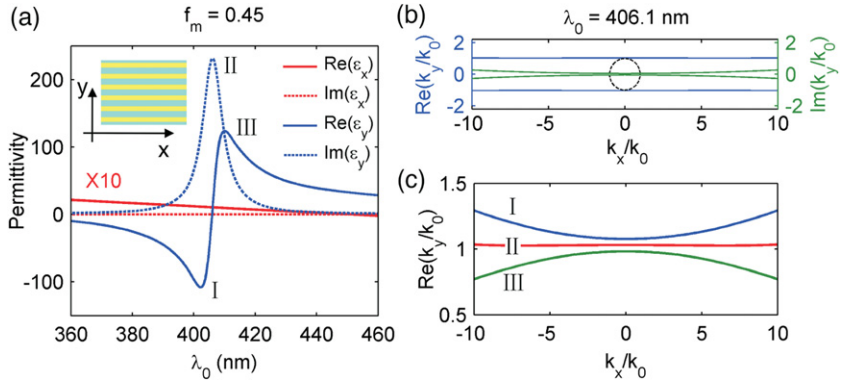

Figure 1. (a) The dependence of the permittivity tensor on the wavelength λ_0 for a metal–dielectric multilayer structure with metal filling ratio $f_m = 0.45$. Re(ε_x) has been scaled up by ten times. The three Roman numbers (I, II, III) indicate the wavelengths corresponding to negatively maximized Re(ε_y), maximized Im(ε_y) and maximized Re(ε_y), respectively. The inset shows the multilayer structure with Ti_3O_5 (green color) and silver (yellow color). (b) The IFC at the resonance wavelength $\lambda_0 = 406.1$ nm (at position II). Re(k_y) and Im(k_y) are represented by the blue and green lines, respectively. Although Im(k_y) grows with transverse wavevector k_x (ranges from $0.0476k_0$ to $0.2674k_0$ as k_x increases from 0 to $10k_0$), it remains small due to the large magnitude of ε_y, which gives a low propagation loss. The dashed black circle is the IFC of air. (c) The IFCs for the three wavelengths indicated in (a). The flattest IFC is obtained at the resonance wavelength with maximized Im(ε_y).

where ε_d and ε_m are the permittivities of titanium oxide and silver, and f_d and f_m ($f_d + f_m = 1$) are the filling ratios of titanium oxide and silver, respectively. The silver filling ratio f_m is 0.45, and its permittivity is taken from the experimental results [13]. The dependence of the permittivity tensor on wavelength λ_0 is shown in figure 1(a), which is calculated using equation (1) according to the effective medium theory. It is found that the longitudinal permittivity component ε_y shows a strong resonance at $\lambda_0 = 406.1$ nm (at position II), where Im(ε_y) has a peak of more than 230, while Re(ε_y) flips its sign quickly across the resonance from negative maximum (at position I) to positive maximum (at position III). Previously, ultra-large Re(ε_y) (at position III) has been utilized to realize subwavelength beam propagation without diffraction [4, 5]. However, the behavior of ultra-high Im(ε_y) has not been considered before. It is intuitively thought that a large Im(ε_y) will increase the beam propagation loss. In contrast, it will be demonstrated that the extreme loss-anisotropy with an ultra-large imaginary part can enable low-loss diffraction-free subwavelength beam propagation. For TM-polarized light with non-vanishing E_x, E_y and H_z field components, the corresponding IFC is determined by

$$k_x^2/\varepsilon_y + k_y^2/\varepsilon_x = k_0^2, \tag{2}$$

where k_x is the transverse k-vector and k_y is the propagation k-vector. Figure 1(b) shows that an ultra-flat IFC over a large k_x range is supported at the resonance wavelength $\lambda_0 = 406.1$ nm (position II), with $\varepsilon_x = 1.06 + 0.098\mathrm{i}$ and $\varepsilon_y = 10.48 + 231.70\mathrm{i}$. The propagation k-vector Re(k_y) remains a constant for all different k_x, while the imaginary part of the propagation k-vector Im(k_y) is quite small. To understand the behavior of the flat IFC, equation (2) can be rewritten as

$$k_y = \sqrt{\varepsilon_x\left(k_0^2 - \frac{k_x^2}{\varepsilon_y}\right)} \approx \sqrt{\varepsilon_x}k_0 - \sqrt{\varepsilon_x}\frac{k_x^2}{2k_0\varepsilon_y}, \tag{3}$$

where the approximation $|\varepsilon_y| \gg 1$ has been used to derive the above formula. Since ε_x is dominated by its real part, and ε_y is dominated by its imaginary part at the resonance wavelength, Re(k_y) $\approx \sqrt{\varepsilon_x}k_0$ and Im(k_y) $\approx \sqrt{\varepsilon_x}k_x^2/\left(2k_0\,\mathrm{Im}(\varepsilon_y)\right)$, which shows that Re($k_y$) is independent of k_x and Im(k_y) is weakly proportional to k_x^2. Moreover, the propagation loss Im(k_y) is inversely proportional to Im(ε_y) and the large material loss Im(ε_y) actually enables the low-loss beam propagation. The ultra-large Im(ε_y) in extremely loss-anisotropic metamaterial not only gives rise to an ultra-flat IFC over a broad k_x range, but also results in ultra-small beam propagation loss.

To further illustrate the importance of large Im(ε_y), the comparisons of IFC curves at three different wavelengths of I, II and III are shown in figure 1(c), which corresponds to negatively maximized Re(ε_y), maximized Im(ε_y) and maximized Re(ε_y), respectively. This indicates that the maximized Im(ε_y) case results in the flattest IFC with almost zero curvature, while the other two IFCs show positive and negative curvatures, respectively. These behaviors can be clearly understood using equation (3), in which a purely real ε_y will contribute to Re(k_y) and influence the curvature of the IFC (a positive ε_y leads to a negative curvature and vice versa). It is clear that the maximized Im(ε_y) case with zero curvature will achieve diffraction-free subwavelength beam propagation.

Next, diffraction-free deep subwavelength beam propagation will be demonstrated from a numerical simulation based on the finite element method (FEM). Here, it is worthwhile to define the minimal waist size of the light beam which can propagate inside the multilayer structure without diffraction. It is known from equation (2) that $k_x^2/\varepsilon_y \ll k_0^2$ is required to obtain a nearly flat IFC, thus the minimal beam waist size $w_{\min}$ turns out to be $2\pi/\max(k_x) = \lambda_0\sqrt{|\varepsilon_y|}$. Figure 2 shows the propagation of ultra-narrow Gaussian beams (with a waist size of 40 nm $\sim 0.1\lambda_0 > w_{\min}$) inside loss-anisotropic metamaterials with different geometries at

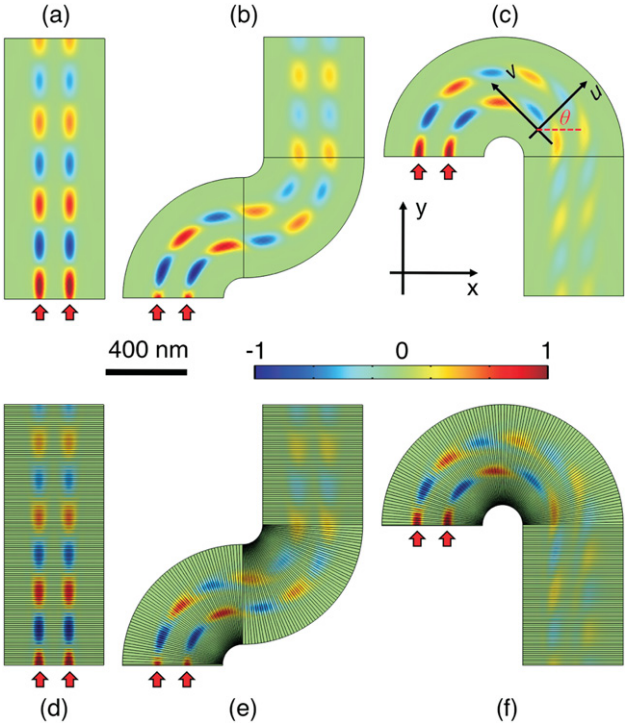

Figure 2. Diffraction-free deep subwavelength beam propagation in extremely loss-anisotropic metamaterials. The distributions of magnetic field H_y are shown in (a)–(c) for an ideal effective medium and (d)–(f) for a multilayer structure with period $a = 20$ nm. (a), (d) Straight beam propagation. (b), (e) 90° beam bending. (c), (f) 180° beam bending. The center-to-center distance of the two beams is 150 nm in all the simulations.

the resonance wavelength $\lambda_0 = 406.1$ nm. The effective medium results and the realistic multilayer results are shown in figures 2(a)–(c) and (d)–(f), respectively. Figures 2(a) and (d) show that ultra-narrow Gaussian beams can propagate over a long distance without any wavefront distortion. Two subwavelength beams with 150 nm center-to-center distance remain well defined as the beams propagate across the multilayer from the bottom to the top. It is emphasized that the subwavelength beam confinement is entirely due to the unique loss-anisotropic property, and the beam path is solely determined by the launching location. This is distinct from the situation in a subwavelength waveguide, where the mode is confined by the waveguide boundary.

Besides the straight beam propagation, the flow of light can be flexibly modeled by controlling the local metamaterial properties. For instance, the beam path can be manipulated by gradually varying the direction of multilayers, since the direction of beam propagation is always vertical to the multilayer interface. The designed geometries for achievement of 90° and 180° bending of subwavelength beams are shown in figures 2(b)–(c) and (e)–(f), for both the effective media and the multilayer structure. In the effective medium calculation, the anisotropic permittivity tensor depends on the tilted angle of the multilayer interface. In the local coordinate (u, v), the components of the permittivity tensor can still be determined by the mixing formula in equation (1). The permittivity tensor expression in the global coordinate (x, y) is related to that in the local coordinate as

$$\overleftrightarrow{\varepsilon}(x, y) = \begin{pmatrix} \varepsilon_u \cos^2\theta + \varepsilon_v \sin^2\theta & (\varepsilon_u - \varepsilon_v)\sin\theta\cos\theta \\ (\varepsilon_u - \varepsilon_v)\sin\theta\cos\theta & \varepsilon_u \sin^2\theta + \varepsilon_v \cos^2\theta \end{pmatrix}, \quad (4)$$

where θ is the local tilted angle of the multilayer with respect to the $+x$ axis, and ε_u and ε_v are the local permittivity tensor components along and normal to the multilayer, respectively. The simulation results indicate that the flow of light can indeed be manipulated while maintaining the deep subwavelength beam confinement and diffraction-free propagation. For the results of 180° bending shown in figures 2(c) and (f), it is noted that the wavefront becomes tilted at the output section (but the energy flow is still vertical to the interface as a result of the flat IFC). This is due to the fact that the light traveling at the inner side undergoes a shorter optical path than the light traveling at the outer side. The phase difference arising from the light path difference leads to the beam wavefront tilting.

Figure 2 shows that the multilayer structure simulation results agree very well with the EMT results, indicating that the multilayer structure with period $a = 20$ nm ($f_m = 0.45$) can represent the loss-anisotropic effective medium well. However, the fabrication of such thin layers is very challenging in reality (but possible [14]). It is interesting to study the properties of a metal–dielectric multilayer with a large period a, where the nonlocal effect has to be taken into account [15]. The dispersion relation describing the realistic multilayer structure for TM-polarized light is

$$\cos\left[k_y(a_m + a_d)\right] = \cos(k_m a_m)\cos(k_d a_d) - \gamma_{TM}\sin(k_m a_m)\sin(k_d a_d), \quad (5)$$

which is derived by treating the layered structure as a one-dimensional photonic crystal. Here, $\gamma_{TM} = (\varepsilon_d k_m/\varepsilon_m k_d + \varepsilon_m k_d/\varepsilon_d k_m)/2$, $k_m = \sqrt{\varepsilon_m k_0^2 - k_x^2}$, and $k_d = \sqrt{\varepsilon_d k_0^2 - k_x^2}$. The IFCs corresponding to a realistic multilayer structure with $a = 40$ nm are shown in figure 3(a). It is found that the IFC curve at $\lambda_0 = 406.1$ nm is no longer flat due to the nonlocal effect. That is to say, the effective permittivity tensor becomes strongly wavevector dependent, so that the permittivity components ε_x and ε_y will be functions of not only the frequency but also the k-vector. The frequency corresponding to the flattest IFC will then be shifted. For the multilayer structure with $a = 40$ nm, it turns out that the flattest IFC occurs at $\lambda_0 = 418.3$ nm (which can be mathematically determined by finding the working wavelength with zero IFC curvature), as shown in figure 3(a). The propagation of subwavelength Gaussian beams at the two wavelengths in the multilayer structure with $a = 40$ nm is shown in figure 3(b). As can be expected from the IFC curves in figure 3(a), the Gaussian beams at $\lambda_0 = 406.1$ nm suffer strong diffraction, resulting in distorted beam profiles. In comparison, the beam profiles remain well defined for the Gaussian beams at $\lambda_0 = 418.3$ nm.

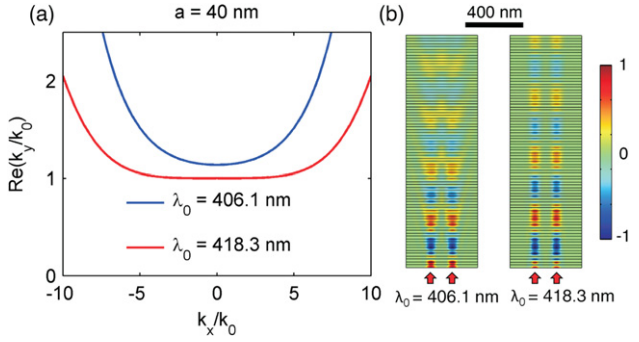

Figure 3. (a) The IFCs for a realistic multilayer structure with $a = 40$ nm at two different wavelengths. (b) The Gaussian beam propagation at the two wavelengths. Diffraction-free beam propagation is achieved after taking into account the nonlocal effect induced wavelength shift.

3. Conclusion

In conclusion, extremely loss-anisotropic metamaterial is designed using metal–dielectric multilayer structures. The IFC corresponding to such metamaterial turns out to be ultra-flat over a broad k-vector range. This unique property is then utilized to obtain diffraction-free deep subwavelength beam propagation. Furthermore, it is shown that the propagation of light beams can be manipulated flexibly by tuning the direction of the multilayer structure. Moreover, the nonlocal effect occurring in multilayer structures with large multilayer periods is investigated. It is found that diffraction-free beam propagation is still possible after taking into account the nonlocal effect. This study is very attractive for many applications such as optical imaging, optical integration, and on-chip optical communication.

Acknowledgments

This work was partially supported by the Department of Mechanical and Aerospace Engineering and the Intelligent Systems Center at Missouri S&T, the University of Missouri Research Board, the Ralph E Powe Junior Faculty Enhancement Award, and the National Natural Science Foundation of China (61178062 and 60990322).

Y He and L Sun contributed equally to this work.

References

[1] Shin J, Shen J T and Fan S 2009 Three-dimensional metamaterials with an ultrahigh effective refractive index over a broad bandwidth *Phys. Rev. Lett.* **102** 093903

[2] Choi M, Lee S H, Kim Y, Kang S B, Shin J, Kwak M H, Kang K Y, Lee Y H, Park N and Min B 2011 A terahertz metamaterial with unnaturally high refractive index *Nature* **470** 369–73

[3] Han S, Xiong Y, Genov D, Liu Z, Bartal G and Zhang X 2008 Ray optics at a deep-subwavelength scale: a transformation optics approach *Nano Lett.* **8** 4243–7

[4] Catrysse P B and Fan S 2012 Deep sub-wavelength beam propagation, beam manipulation and imaging with extreme anisotropic meta-materials *Proc. Quantum Electronics and Laser Science Conf. (San Jose, California, 6 May 2012)* QTu1G (doi:10.1364/QELS.2012.QTu1G.7)

[5] Catrysse P B and Fan S 2011 Transverse electromagnetic modes in aperture waveguides containing a metamaterial with extreme anisotropy *Phys. Rev. Lett.* **106** 223902

[6] Yao J, Liu Z, Liu Y, Wang Y, Sun C, Bartal G, Stacy A M and Zhang X 2008 Optical negative refraction in bulk metamaterials of nanowires *Science* **321** 930

[7] Liu Z, Lee H, Xiong Y, Sun C and Zhang X 2007 Far-field optical hyperlens magnifying sub-diffraction-limited objects *Science* **315** 1686

[8] Krishnamoorthy H N S, Jacob Z, Narimanov E, Kretzschmar I and Menon V M 2012 Topological transitions in metamaterials *Science* **336** 205–9

[9] Cui Y, Fung K H, Xu J, Ma H, Jin Y, He S and Fang N X 2012 Ultrabroadband light sbsorption by a sawtooth anisotropic metamaterial slab *Nano Lett.* **12** 1443–7

[10] He Y, He S, Gao J and Yang X 2012 Nanoscale metamaterial optical waveguides with ultrahigh refractive indices *J. Opt. Soc. Am.* B **29** 2559–66

[11] Yang X, Yao J, Rho J, Yin X and Zhang X 2012 Experimental realization of three-dimensional indefinite cavities at the nanoscale with anomalous scaling laws *Nature Photon.* **6** 450–4

[12] Rho J, Ye Z, Xiong Y, Yin X, Liu Z, Choi H, Bartal G and Zhang X 2010 Spherical hyperlens for two-dimensional sub-diffractional imaging at visible frequencies *Nature Commun.* **1** 143

[13] Johnson P B and Christy R W 1972 Optical constants of the noble metals *Phys. Rev.* B **6** 4370–9

[14] Chen W, Thoreson M D, Ishii S, Kildishev A V and Shalaev V M 2010 Ultra-thin ultra-smooth and low-loss silver films on a germanium wetting layer *Opt. Express* **18** 5124–34

[15] Elser J, Podolskiy V A, Salakhutdinov I and Avrutsky I 2007 Nonlocal effects in effective-medium response of nanolayered metamaterials *Appl. Phys. Lett.* **90** 191109